Clays and Clay Minerals, Vol. 66, No. 1, 74–85, 2018.

FORMATION OF NH_4-ILLITE-LIKE PHASE AT THE EXPENSE OF DIOCTAHEDRAL VERMICULITE IN SOIL AND DIAGENETIC ENVIRONMENTS – AN EXPERIMENTAL APPROACH

Michał Skiba[1,*], Stefan Skiba[2], Arkadiusz Derkowski[3], Katarzyna Maj-Szeliga[1], and Beata Dziubińska[1]

[1] Institute of Geological Sciences, Jagiellonian University, 30-387 Kraków, ul. Gronostajowa 3a, Poland
[2] Institute of Geography and Spatial Management, Jagiellonian University, 30-387 Kraków, ul Gronostajowa 7, Poland
[3] Institute of Geological Sciences, Polish Academy of Sciences, 31-002 Kraków, ul. Senacka 1, Poland

Abstract—Selective sorption and/or fixation of cations with low hydration energies (*e.g.* K^+, NH_4^+, Rb^+, Cs^+) by vermiculites is a well known phenomenon in soil science and it has been described by many investigators since the 1950s. Because most of the available studies deal with trioctahedral vermiculites, cation fixation in dioctahedral vermiculites is not as well understood as fixation by trioctahedral structures. The objective of the present study was to investigate the influence of NH_4^+ saturation on the structure of a natural dioctahedral vermiculite. Because no dioctahedral vermiculite standard reference material was available, two natural dioctahedral vermiculite-rich soil clay samples were used in the study. The clays were saturated with NH_4^+ using different protocols to simulate natural processes that likely take place in soils. The degree of NH_4^+ fixation by the dioctahedral vermiculite was evaluated using X-ray diffraction, elemental N analysis, and infrared spectroscopy. All the treatments that involved NH_4^+ saturation caused NH_4^+ fixation and irreversible collapse (*i.e.* contraction to ~10 Å) of at least a portion of the previously hydrated (vermiculitic) interlayers. Air drying of the NH_4^+-saturated samples greatly enhanced the degree of the collapse. The results indicated that the collapse of dioctahedral vermiculite leads to the formation of a NH_4-illite-like phase that is likely to occur in some soils and sediments that are rich in organic matter. The formation of a NH_4-illite-like phase by NH_4^+ fixation in vermiculitic interlayers needs to be taken into consideration in studies that deal with the clay mineralogy of sedimentary basins.

Key Words—Ammonium Illite, Dioctahedral Vermiculite, Early Diagenetic Illitization, NH_4^+-fixation, Soil Illitization.

INTRODUCTION

Fixation of NH_4^+ by soil materials is a well-known phenomenon (*e.g.* Douglas, 1989 and cited literature; Nieder *et al*., 2011 and cited literature). It has been studied extensively, mainly in the context of NH_4-based N-fertilization and on N availability for crops and on microflora. NH_4^+ can be produced during organic matter decomposition (Nieder *et al*., 1995) both in soils and in organic-rich, soil-derived fresh-water and marine sediments during early diagenesis. Because of those reasons, NH_4^+ fixation is likely to take place due to natural processes both in soil and in diagenetic environments. According to Douglas (1989), Nieder *et al*. (2011), and Matocha *et al*. (2016), 2:1 clay minerals (*i.e.* illite, smectite, and vermiculite) play a crucial role in NH_4^+ fixation. In illite and illite-containing mixed-layer clay minerals, NH_4^+ is fixed within the so-called frayed edges, whereas smectite and vermiculite are believed to accommodate NH_4^+ within the interlayer space. The penetration of NH_4^+ into the interlayer space causes the clay layers to collapse to ~10 Å because of the low hydration energy of NH_4^+. Several mineralogical studies that have dealt with the fixation of low hydration-energy cations (*i.e.* NH_4^+ and K^+) by dioctahedral smectites have been published (*e.g.* Eberl *et al*., 1986; Šucha and Širáňová, 1991; Shen and Stucki, 1994; Heller-Kallai and Eberl, 1997; Stucki, 2011). According to those papers, the fixation within smectite interlayers occurs only when NH_4^+-saturated or K^+-saturated smectites are subjected to repeated wetting and drying (WD) cycles or when octahedral Fe(III) in the structure has been reduced to Fe(II). Without the application of WD cycles or the reduction of octahedral Fe(III), the collapse is completely reversible and the smectites can be exchanged and re-expanded using standard laboratory protocols by cations with higher hydration energies like Na^+, Sr^{2+}, Mg^{2+}, or Ca^{2+} (Eberl *et al*., 1986; Shen and Stucki, 1994; Stucki, 2011). Considerably less attention has been devoted to NH_4^+ fixation by dioctahedral vermiculite despite the fact that dioctahedral vermiculite is a common mineral in soil and weathering environments.

The selective sorption and/or fixation of cations with low hydration energies (*e.g.* K^+, NH_4^+, Rb^+, Cs^+) by vermiculites has been known to soil scientists for many years, as reported by many investigators since the 1950s (Rich and Obenshein, 1955; Douglas, 1989 and cited literature). Most of the available published studies dealt

* E-mail address of corresponding author:
michal.skiba@uj.edu.pl
DOI: 10.1346/CCMN.2018.064082

with trioctahedral vermiculites and, as a consequence, cation fixation in dioctahedral vermiculites is not as well understood as fixation in trioctahedral structures.

Dioctahedral vermiculite is a swelling 2:1 phyllosilicate that has a 0.6–0.9 negative layer charge per half unit cell (*i.e.* close to that of interlayer-deficient mica-illite) (Guggenheim *et al*., 2006). In contrast to illite, which has interlayers that are occupied by anhydrous K^+ and/or NH_4^+, dioctahedral vermiculites have interlayers that are occupied by hydrated exchangeable cations (*e.g.* Mg^{2+}, Na^+, *etc*.). Dioctahedral vermiculites occur in soils and in fresh water sediments (*e.g.* Środoń, 1999) where it is always associated with quite a complex mixture of other clay minerals that includes mixed layer phases (*e.g.* Skiba, 2013; Viennet *et al*., 2015). Because of that fact, a determination of the layer charge of dioctahedral vermiculites in natural samples is very difficult. In the routine analysis of soils and fresh water sediments, the identification of dioctahedral vermiculite is performed using X-ray diffractometry (XRD) and it is based on operational definitions (Bailey, 1980; Brown and Brindley, 1980; Środoń and Gaweł, 1988). According to those definitions, vermiculite (just like smectite) gives (001) peaks of ~14 Å and ~12.5 Å for air-dry Mg^{2+}-saturated and Na^+-saturated forms, respectively. This is believed to be due to the fact that Mg-saturated dioctahedral vermiculite accommodates two layers of water within the interlayer space, while Na-saturated dioctahedral vermiculite accommodates only one layer. Unlike smectites, the ~14 Å peak of Mg-saturated dioctahedral vermiculites do not shift to lower angles after the sample is solvated with glycerol, while the ~12.5 Å peak of Na-dioctahedral vermiculites moves to ~14 Å after solvation with ethylene glycol.

The available published studies that illustrate cation fixation by dioctahedral minerals (*e.g.* Rich and Obenshein, 1955; Rich, 1964; Rich and Black, 1964; Dolcater *et al*., 1972), however, indicate that dioctahedral vermiculites appear to selectively sorb and fix K^+ and NH_4^+ in a manner similar to trioctahedral vermiculites.

Saturation of dioctahedral vermiculite with NH_4^+ is likely to collapse the interlayers and lead to the formation of a ~10 Å NH_4-illite (tobelite) - like phase. Tobelite is an interlayer-cation-deficient dioctahedral mica similar to illite. Unlike illite, which has interlayers mainly occupied by fixed K^+, tobelite mainly contains NH_4^+ in the interlayers. Środoń *et al*. (1992, 2009) determined that illite layer charge is close to that of true micas (*i.e*. 0.89, 0.94), while the layer charge range for aluminous illite is 0.6–0.9 according to Guggenheim *et al*. (2006). This range precisely covers the theoretical range in dioctahedral vermiculite layer charge. Tobelite, an end-member NH_4-illite that is common in hydrocarbon reservoir rocks, has often been found to have a micaceous layer charge component that is much lower than true micas and as low as 0.75–0.81 (Drits *et al*., 1997; Drits *et al*., 2005; Mesto *et al*., 2012 and cited references).

The collapse of dioctahedral vermiculite interlayers due to NH_4^+ saturation is expected to be irreversible to the ion exchange procedures (Jackson, 1969) routinely used to prepare clays for mineralogical studies. The XRD-mineralogy of this NH_4^+ interlayer reaction in natural dioctahedral-vermiculite bearing clays has apparently not been well documented in the available published literature. In a previous work, Skiba (2013) showed that a dioctahedral vermiculite from a podzol (spodosol) indeed irreversibly collapsed at room temperature to an illite-like phase after it was saturated with K^+. The observed collapse indicated that the process of K^+ fixation that leads to dioctahedral vermiculite contraction ("illitization") very likely occurs in soils, weathering environments (*e.g.* due to local fluctuations in K^+ concentrations), and during early diagenesis of marine sediments.

The aim of the present study was: (1) to find out if natural dioctahedral vermiculites indeed collapse irreversibly to a NH_4-illite-like phase when saturated with NH_4^+, (2) to determine whether or not collapse is likely to occur in natural soil and diagenetic environments, and (3) to find out if the collapse may occur under wet conditions or if the NH_4^+-saturated dioctahedral vermiculite must be dried for the collapse to occur.

MATERIALS AND METHODS

Materials and experiments

For the purpose of the present study, natural soil clays were used. The samples were collected from the albic horizons of two podzols (spodosols) that developed on granitic parent material in the Tatra Mountains, Poland. Sample 1E came from a Haplic Podzol (Haplorthod) developed in the Dolina Suchej Wody Valley and sample 6E came from a Haplic Podzol developed on Trzydniowiański Wierch Mountain. Finding appropriate soil samples for the planned experiment was challenging. This was because of the fact that dioctahedral vermiculite in most published studies was identified based only on the behavior of the strongest (*i.e*. (001)) XRD reflection. This identification method makes the distinction between discrete dioctahedral vermiculite and mixed layer phases impossible. The potential presence of hydroxy interlayering (*e.g*. Barnishel and Bertsch, 1989) and intercalation by soil organic matter (*e.g*. Brown 1953; Skiba *et. al*., 2011) make the task even more complicated. In a previous study, Skiba (2013) examined the XRD data in previously published research and in XRD analyses of a vast number of soil clays, which led to the conclusion that the existence of dioctahedral vermiculite as a discrete mineral phase is doubtful. Because of that conclusion, two Na^+-saturated soil clay (*i.e* <2 μm) fractions that were rich in dioctahedral mica-vermiculite mixed layer minerals were used in the experiments.

https://doi.org/10.1346/CCMN.2018.064082 Published online by Cambridge University Press

Samples 1E and 6E both contained R0 and R1 (Reichweite layer stacking probability) dioctahedral mica-vermiculite minerals, but sample 1E also contained some R0 mica-vermiculite-smectite minerals. Both of the samples contained kaolinite, discrete illite, and traces of quartz (Skiba, 2007, 2013). The dioctahedral aluminous nature (clearly different from trioctahedral vermiculites) was indicated by the position of the 060 reflection at ~1.50 Å in the XRD patterns and by the presence of a strong band at 3624 cm^{-1} in the OH-stretching region of the FTIR spectra (Skiba, 2007). More details on the soil origin, the properties, and the mineralogy of the clays were given by Skiba (2007, 2013) and Skiba and Skiba (2005).

Unless specified differently, all chemical treatments applied in the present study used analytical reagent-grade chemicals (Polskie Odczynniki Chemiczne (POCH S.A.), Gliwice, Poland). The clay fractions were separated according to the procedure described by Jackson (1969). Aliquots of soil samples were first treated with H_2O_2 buffered with pH = 5.5 Na-acetate buffer prepared using deionized water (Labopol-Polwater, Krakow, Poland) and reagent-grade chemicals to remove organic matter. Free Fe oxide removal from the samples was performed according to the procedure of Mehra and Jackson (1958). In the last step, the samples were Na-saturated by repeated washing with 1 M NaCl solution. Clay fractions were separated from the pre-treated samples using a Thermo Sorvall ST40 centrifuge (Thermo Fisher Scientific Inc., Waltham, Massachusetts, USA) equipped with a swinging-bucket rotor. The separated clays were flocculated using NaCl and dialyzed using Nadir®-dialysis tubing (Carl Roth GmbH+Co. KG, Karlsruhe, Germany) until a conductivity of <1 $\mu S \cdot cm^{-1}$ was reached. The obtained suspensions were vigorously stirred and split into small portions that contained ~300 mg of clay each. Four portions of the clay fractions from each sample were obtained and were used in the experiments (Table 1).

Three portions of each Na^+-saturated sample (samples (1E)_NH_4_Na and (6E)_NH_4_Na) were NH_4^+ saturated by repeated washes (four times) using 1 M NH_4Cl solution. One portion was dialyzed and used to examine the effects of NH_4^+ saturation on dioctahedral vermiculite structure; the second portion was immediately (*i.e.* without drying) re-saturated with Na^+ and dialyzed; and the third portion was air dried at room temperature (~20ºC) for ~48 h, redispersed in DI water, Na^+- saturated, and dialyzed.

The final Na^+ saturation was performed in each case using an acetate buffer treatment (1 h at 90ºC) and four 1 M NaCl solution washes followed by dialysis. The acetate buffer treatment was used because it appeared to be more efficient for Na^+ saturation than washing with 1 M NaCl and because it is the first step in the chemical pre-treatments recommended for the separation of clay fractions from natural samples (Jackson, 1969).

Table 1. Treatment codes, sample symbols, experimental treatments, measured C and N concentrations, and selected parameters used for the XRD patterns and the FTIR spectra.

Treatment code	Sample symbol	Treatment used	%N	%C	001 XRD[a] (Å)	NH_4 FTIR[b] 1430 cm^{-1} area	NH_4 FTIR[c] ~3300 cm^{-1} area	NH_4 FTIR[d] Si-O env. area
1	(1E)_Na	Na^+ saturation	0.26	9.38	13.28	120	133	14175
2	(1E)_NH_4	NH_4^+ saturation	0.91	10.76	11.74	877	1695	15544
3	(1E)_NH_4_Na	NH_4^+ saturation + Na^+ saturation	0.36	9.97	13.06	182	330	14650
4	(1E)_NH_4_D_Na	NH_4^+ saturation + air-drying + Na^+ saturation	0.44	9.78	12.60	305	571	15012
1a	(6E)_Na	Na^+ saturation	0.26	9.30	11.69	102	113	12500
2a	(6E)_NH_4	NH_4^+ saturation	0.71	9.56	10.98	627	1200	14350
3a	(6E)_NH_4_Na	NH_4^+ saturation + Na^+ saturation	0.38	9.13	11.45	225	350	14250
4a	(6E)_NH_4_D_Na	NH_4^+ saturation + air-drying + Na^+ saturation	0.48	9.40	11.41	415	660	14700

[a] Mean (weighted average) 001 XRD peak position measured for ethylene glycol-solvated mounts.
[b] Area of bands near 1430 cm^{-1} given in arbitrary units.
[c] Area of bands near 3300 cm^{-1} given in arbitrary units.
[d] Area of Si-O bands near 1030 cm^{-1} given in arbitrary units.

https://doi.org/10.1346/CCMN.2018.064082 Published online by Cambridge University Press

Analytical methods

The collapse of the dioctahedral vermiculite due to NH_4^+ fixation was studied using X-ray diffractometry (XRD) (Philips X'Pert APD, Philips Electronics N.V., Almelo, The Netherlands). Fourier-transform infrared spectroscopy (FTIR) (Bio Rad FTS 135, Bio-Rad Laboratories, Cambridge, Massachusetts, USA) and elemental (*i.e.* N) analyses (Vario El III, Elementar Analysensysteme GmbH, Langenselbold, Germany) were used to estimate NH_4 fixation. Oriented clay mounts with a surface density of ~10 mg/cm^2 clay were prepared by re-suspending the samples in deionized water and depositing the clays on glass petrographic slides. XRD analyses were performed using a Philips X'Pert diffractometer with a vertical goniometer PW3020, equipped with a 1º divergence slit, a 0.2-mm receiving slit, incident and diffracted beam Soller slits, a 1º anti-scatter slit, and a graphite diffracted-beam monochromator. CuKα radiation was used with a tube voltage and current of 40 kV and 30 mA. The air-dried mounts were scanned from 2 to 52º2θ with a counting time of 2 s per 0.02º step under ambient humidity (~40% – 50% RH) and after ethylene glycol vapor (analytical reagent grade, POCH S.A., Gliwice, Poland) solvation (12 h at 60ºC). The N and C concentrations in the studied clays were measured using a Vario El III elemental CHNS analyzer (Elementar Analysensysteme GmbH, Langenselbold, Germany). Prior to the analyses, the samples were dried overnight at 105ºC, packed into Sn foil (Elementar Analysensysteme GmbH, Langenselbold, Germany), and pressed. Sulfanilic acid (standard for elemental analysis, Merck, Darmstadt, Germany) was used to prepare standard curves for both C and N determinations. The FTIR spectra were collected for clays dispersed in KBr pellets (FTIR grade, Sigma-Aldrich Chemie, Steinheim, Germany) using a Bio Rad FTS 135 FTIR spectrometer (Bio-Rad Laboratories, Cambridge, Massachusetts, USA) operated under a dry N_2 atmosphere. Thirty-two scans were collected for each sample in the 400 to 4000 cm^{-1} range with a resolution of 2 cm^{-1}. The pellets (0.8 mg clay/300 mg KBr or 1.5 mg/300 mg KBr) were prepared using clay samples that had been dried by heating at 105ºC for 24 h and with KBr powder that was dried by heating at 550ºC for 24 h. After the collection of FTIR spectra, the pellets were heated again at 150ºC overnight and second sets of spectra were collected.

A detailed and precise XRD pattern simulation for multi-component (illite-smectite-vermiculite) interstratified soil clay systems that were formed by several populations with different stacking orders (Skiba, 2013) and with the different properties of layers saturated with NH_4^+ or Na^+ and solvated by water and ethylene glycol is an enormously complex and difficult task (Skiba, 2013; Viennet *et al*., 2015). Because of the difficulty of this task, the weighted-average position of the major 2:1 layer clay composite 001 reflections at ~6.1−8.2º2θ CuKα were calculated for each Na-saturated and ethylene glycol-saturated sample and was used as a proxy for NH_4^+ fixation (Table 1). To better compare the XRD results obtained in the present study to XRD results previously presented by Skiba (2013), whole-pattern, multi-specimen modeling was performed for the Na (1E)_NH_4_Na and (1E)_NH_4_D_Na sample XRD patterns. The modeling was performed using the algorithms described by Drits and Sakharov (1976) and implemented into the proprietary software *SYBILLA* (version 2.0_Sept 4, 2009), which belongs to Chevron® and was applied using the same procedures and structural parameters described by Skiba (2013). To calculate the XRD patterns, the Na^+-saturated sample models by Skiba (2013) were taken as starting models. In the course of the modeling, the initial structural parameters were kept constant for all the phases except for the mixed-layer phases that contained vermiculite and/or smectite. The starting models for mixed-layer phases that contained vermiculite were modified by the addition of tobelite layers (assuming the mean layer-to-layer distance was 10.33 Å) in order to obtain the best possible fit with the experimental XRD patterns. An attempt was made to obtain a similar concentration (in all the models) for discrete kaolinite, illite, and the individual mixed-layer phases. The concentrations of K-illite-like phases (%I) and tobelite-like phases (%T) were calculated for samples by using formula 2 (%I) and formula 3 (I concentration) from Skiba (2013) for the models. The quality of the fit (R_p) was calculated according to the Howard and Preston (1989) formula (formula 1 (R_p) in Skiba, 2013).

RESULTS

The starting materials used in the present study were from the same bulk samples that were described in detail and used by Skiba (2007, 2013), which precisely simulated air-dry and ethylene glycol solvated, Na-saturated clay fractions. The XRD patterns of air-dry samples had peaks at ~22.5 Å, ~12.5 Å, ~6 Å, 3.34−3.0 Å, and ~2 Å for sample (1E)_Na and at ~22.5 Å, ~12.5 Å, 11.2 Å, 5.5 Å, 3.34−3.0 Å, and ~2 Å for sample (6E)_Na (Figures 1 and 2). After ethylene glycol solvation, the peaks shifted to ~24 Å, ~14 Å, 5.0−4.5 Å, ~3.3 Å, and ~2 Å (sample (1E)_Na) and to ~24.5 Å, ~14 Å, ~12.2 Å, ~4.8 Å, and ~2 Å (sample (6E)_Na) (Figures 1 and 2). According to previous studies (Skiba, 2007, 2013), this behavior indicates that the peaks belong to different random and partly ordered (*i.e.* R0 and R1, respectively) mica-vermiculite and mica-vermiculite-smectite mixed layer minerals. Other peaks observed in both starting materials belong to kaolinite (~7 Å and 3.58 Å), quartz (sharp peaks at 3.34 Å and 4.26 Å), and mica (peaks at 10 Å, 5 Å, 2.5 Å, and ~3.33 Å). The peak at 4.47 Å is the phyllosilicate 02l reflection and indicates a less-than-perfect orientation of the "oriented" clay film. As shown by Skiba

https://doi.org/10.1346/CCMN.2018.064082 Published online by Cambridge University Press

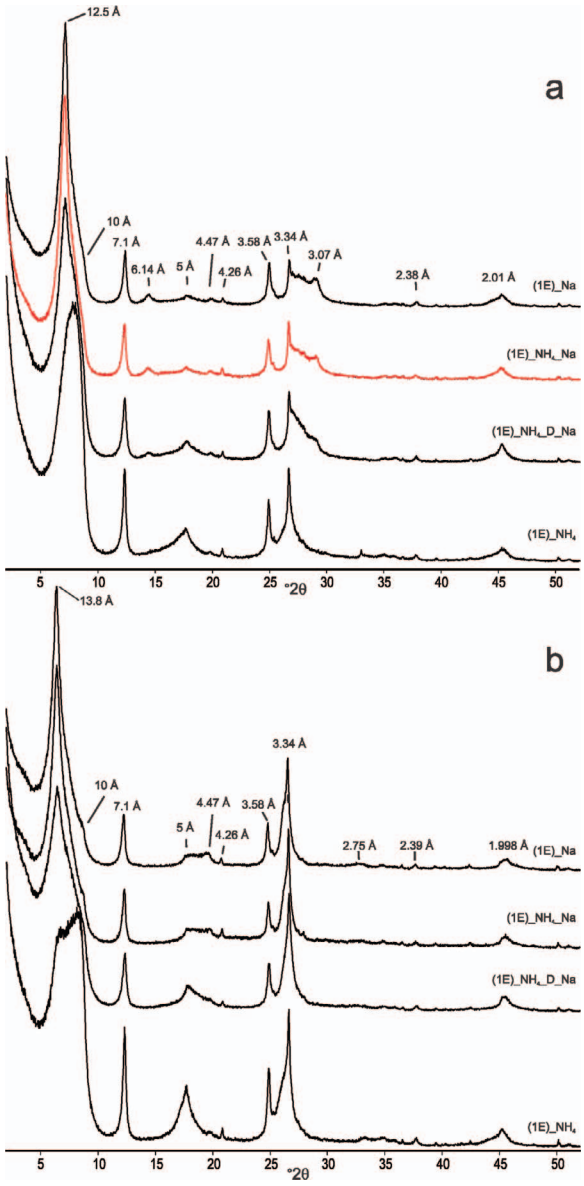

Figure 1. Comparison between the XRD patterns of sample 1E treated using different procedures (Table 1): (a) air-dried sample and (b) ethylene glycol-solvated sample.

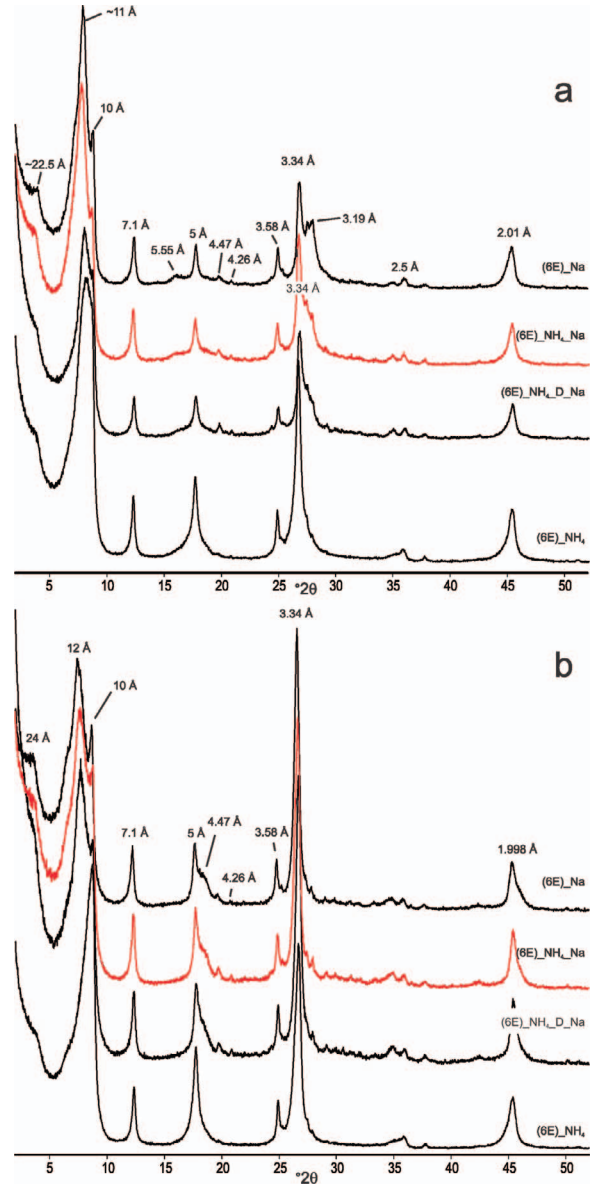

Figure 2. Comparison between the XRD patterns of sample 6E treated using different procedures (Table 1): (a) air-dried sample and (b) ethylene glycol-solvated sample.

(2007), the clays were dioctahedral without detectable concentrations of hydroxy interlayering. The FTIR spectra (Figure 3) of both starting materials were quite similar and showed absorption bands characteristic of kaolinite at 3700 cm^{-1}, 3650 cm^{-1}, 3624 cm^{-1}, 936 cm^{-1}, 915 cm^{-1}, and 700 cm^{-1}. The 2:1 dioctahedral phyllosilicates yielded FTIR absorption bands at 3624 cm^{-1}, 827 cm^{-1}, 750 cm^{-1}, 531 cm^{-1}, and at 470 cm^{-1}, as well as quartz bands at 800 cm^{-1}, 780 cm^{-1}, 531 cm^{-1}, and 470 cm^{-1}. A broad band typical of all silicates was observed at ~1000 cm^{-1}. The bands at 3450 cm^{-1}, 2928 cm^{-1}, 2858 cm^{-1}, 2340 cm^{-1}, and 1735 cm^{-1} were attributed to soil organic matter and decomposition products created by heating overnight at 150ºC (Skiba *et al.*, 2011). Weak bands at ~3300 cm^{-1} and ~1430 cm^{-1} may indicate a small amount of NH_4^+ fixed within 2:1 phyllosilicate interlayers (Ahlrichs *et al.*, 1972; Stone and Wild, 1978; Šucha and Širáňová, 1991), but the band might also be due to soil organic matter (Russell and Fraser, 1994; Skiba *et al.*, 2011).

After NH_4^+-saturation, an increased intensity of the ~10 Å phase XRD reflections was observed in both samples (Figures 1 and 2). This most likely indicates the collapse of the vermiculite interlayers to ~10 Å, which is the characteristic value for illite (Moore and Reynolds, 1997). A low angle shoulder at ~11 Å and the effect of

https://doi.org/10.1346/CCMN.2018.064082 Published online by Cambridge University Press

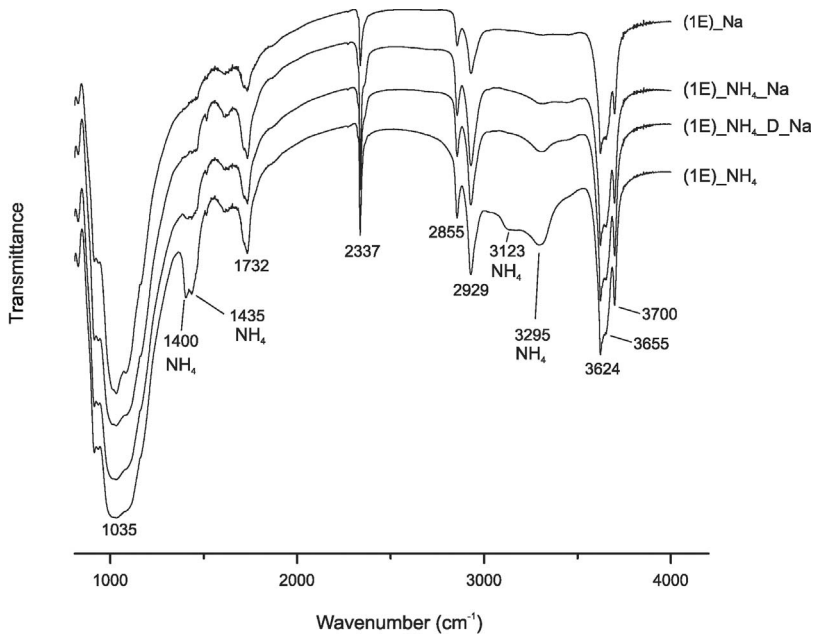

Figure 3. FTIR spectra of sample 1E treated using different procedures (Table 1).

ethylene glycol solvation on the XRD patterns suggested the presence of some hydrated and/or swelling interlayers. In the FTIR spectra of NH_4^+-saturated samples (Figure 3), the bands due to interlayer NH_4^+ (Ahlrichs *et al*., 1972; Stone and Wild, 1978; Šucha and Širáňová, 1991) at ~3300 cm^{-1}, ~1430 cm^{-1}, and ~3124 cm^{-1} were observed.

The XRD patterns of samples that were NH_4^+-saturated, kept moist, and re-saturated with Na^+ showed only small changes relative to the XRD patterns of the initial Na^+-saturated samples. The changes were manifested by an intensity decrease in the low angle reflections relative to the higher angle reflections (Figures 1 and 2) and some intensity increase at the high angle side. This behavior indicated that part of the NH_4^+ was retained after the second Na-exchange saturation and caused a permanent collapse to ~10 Å of at least a small portion of the initially hydrated interlayers in the samples.

The XRD patterns of the samples that were NH_4^+ saturated, air-dried, and re-saturated with Na^+ significantly changed relative to the XRD patterns of the initially Na^+-saturated samples and Na^+-saturated samples that were not dried (Figures 1 and 2). The changes significantly decreased the intensity of the low angle reflections and increased the intensity on the high angle side, which indicated an increase in the content of the ~10 Å phase. The changes indicated that the air-drying step between the NH_4^+ saturation step and the subsequent Na-exchange caused a significant portion of the NH_4^+ to be fixed and led to vermiculite interlayer collapse (Figure 1, Table 1).

The XRD pattern changes produced by the NH_4^+ fixation described above were confirmed by corresponding changes in the FTIR spectra. As the proportion of the ~10 Å phase was increased, the intensities of the NH_4^+ bands at 3100−3450 cm^{-1} and 1400−1450 cm^{-1} seemed to concurrently increase (Figures 3 and 4). When the FTIR bands were normalized to the Si-O envelope area at 850−1300 cm^{-1}, both of the FTIR regions that are characteristic for NH_4^+ were linearly correlated with the N contents (Figure 4), as predicted by Petit *et al*. (1998).

The calculated average XRD peak positions between 6.1−8.22°2θ perfectly matched the N contents in both samples. For a higher N content, the average peak position was lower and shifted toward ~10 Å (Figure 5).

The sample (1E)_NH_4_Na XRD patterns were fitted using the same complex models (containing discrete illite, discrete kaolinite, and seven mixed-layer structures) as the models used in a previous study (Skiba, 2013) to fit the (1E)_Na sample starting material (Table 2, Figure 6). The models fitted to the (1E)_NH_4_Na sample XRD patterns indicated similar concentrations of individual phases as the models used by Skiba (2013) for the (1E)_Na sample; however, an increase in tobelite layers was needed to obtain a satisfactory fit. Kaolinite, illite, and five mixed-layer structures were needed to fit the (1E)_NH_4_D_Na sample XRD patterns.

DISCUSSION

Collapse of interlayers following NH_4^+ saturation.

The saturation of dioctahedral vermiculite with NH_4^+ collapsed the interlayers to ~10 Å or likely to ~10.3 Å, which is typical for a collapsed NH_4^+-smectite or an NH_4-illite (tobelite). Most of the interlayer NH_4^+ was replaced by Na^+ from the Na-acetate buffer and 1 M NaCl treatments, which is a standard procedure commonly

https://doi.org/10.1346/CCMN.2018.064082 Published online by Cambridge University Press

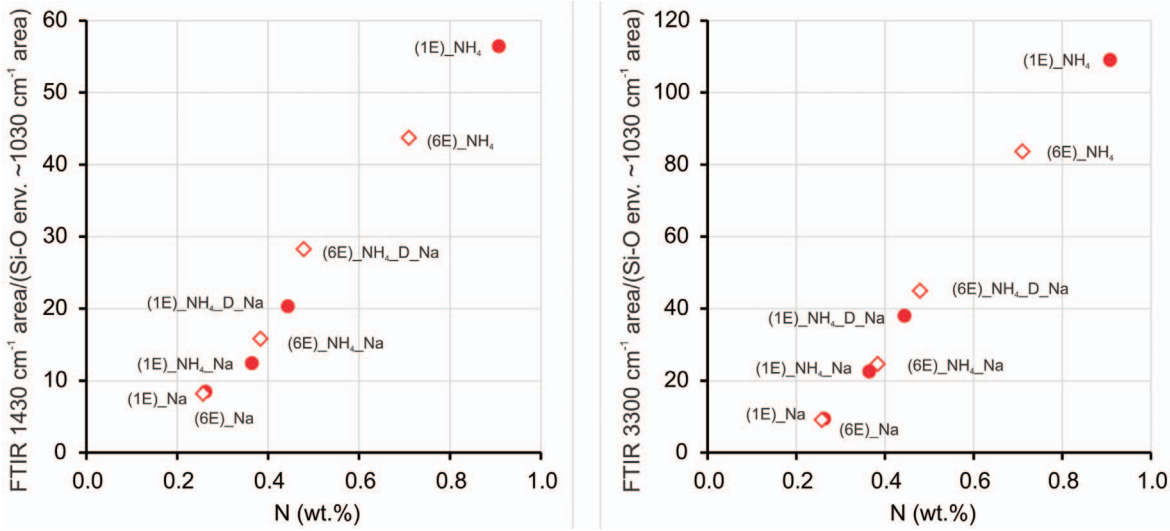

Figure 4. A plot of the FTIR band area that corresponds to the NH_4^+ signals near 1430 cm^{-1} and 3300 cm^{-1} that were normalized to the Si-O envelope area plotted *vs.* the N contents determined using chemical methods. The filled circles = sample 1E and the open diamonds = sample 6E.

used to prepare clay fractions from soils and rocks for analysis (Jackson, 1969), when the NH_4^+-exchanged dioctahedral vermiculite was kept moist. Drying NH_4^+-saturated dioctahedral vermiculite strongly enhanced NH_4^+ fixation and interlayer collapse. Because drying (either air-drying, vacuum-drying, or oven-drying) is almost always used to prepare bulk soil or clay fraction samples, a significant proportion of interlayer NH_4^+ will be fixed if a sample contains any NH_4^+-saturated dioctahedral vermiculite and the fixed NH_4^+ cannot be exchanged by other cations using standard procedures.

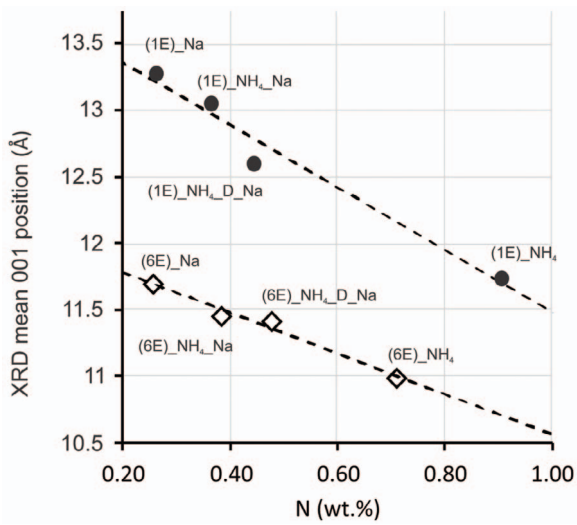

Figure 5. Mean (weighted average) 001 XRD peak position of the Na-saturated and ethylene glycol-solvated specimens plotted against the N content for samples 1E (filled circles) and 6E (open diamonds). The broken lines indicate the trend line.

Because, as was mentioned above, the collapse of dioctahedral vermiculite interlayers to ~10 Å is irreversible (*i.e.* the interlayers cannot be rehydrated and re-opened by Na^+-saturation), the ~10 Å phase formed cannot be distinguished using XRD (and most likely any other method common in mineral characterization) from common illite, in particular from NH_4-illite (10.3 Å).

NH_4^+-fixation vs. K^+-fixation.

The same samples used in the present study were tested for K fixation before using similar sets of experiments, which included a few tests under conditions that match those used in the present study (Skiba, 2013 and Skiba unpublished data). The initial K and N contents of the starting material were subtracted from the K and N contents after K^+ and NH_4^+ saturation. The difference between the initial K and N contents and the K and N contents after K^+ and NH_4^+ saturation should be the K^+ and NH_4^+ cation exchange capacities (CEC) of the initial material, which were 0.46 and 0.48 mmol(+)·g^{-1} for the 1E sample and 0.32 and 0.38 mmol(+)·g^{-1} for the 6E sample, respectively. The CEC values calculated using both methods were in good agreement and consistent with the mineralogical compositions of the clay fractions.

Corresponding experiments using K^+ and NH_4^+ produced a very similar degree of fixation. Both the fraction of fixed cations (expressed as CEC equivalents) and the weighted-average d-spacing calculated using the method in Figure 5 provided matching results (Figure 7). The correlation between fixed K^+ and fixed NH_4^+, however, was not perfectly linear and after the K^+-fixation experiments, fixed K^+ was greater than fixed NH_4^+ (based on chemical methods and the *d* spacings) and the values were closer to mica

https://doi.org/10.1346/CCMN.2018.064082 Published online by Cambridge University Press

Table 2. Structural parameters used for modelling the XRD patterns of the solid products of the experiments using sample 1E.

Sample	Air-dry RH	Rp	Phases air[a]	% of each phase	T mean	EG RH	Rp	Phases Eg[b]	% of each phase	T mean
(1E)_Na	25%	18.76%	Kaolinite	11%	18	32.30%	18.95%	Kaolinite	11%	18
			I-V R0 (3:97)	9%	10			I-V R0 (4:96)	7%	10
			I-V R0 (20:80)	6%	10			I-V R0 (20:80)	6%	10
			I-V-S R0 (3:69:28)	4%	10			I-V-S R0 (3:76 :21)	3%	10
			I-V R0 (40:60)	12%	10			I-V R0 (40:60)	13%	10
			I-V R0 (61:39)	8%	10			I-V R0 (61:39)	7%	10
			I-V R0 (83:17)	35%	10			I-V R0 (80:20)	38%	10
			Illite	9%	14			Illite	9%	14
			I-V R1 (60:40)	6%	10			I-V R1 (60:40)	6%	10
(1E)_NH_4_Na	18.9%	16.69%	Kaolinite	11%	18	21.9%	22.79%	Kaolinite	10%	18
			I-T-V R0 (3:1:96)	10%	10			I-T-V R0 (3:1:96)	7%	10
			I-T-V R0 (20:12:68)	8%	10			I-T-V R0 (20:12:68)	8%	10
			I-T-V-S R0 (3:10:63:24)	8%	10			I-T-V-S R0 (3:10:63:24)	7%	10
			I-T-V R0 (40:11:49)	7%	10			I-T-V R0 (40:11:49)	9%	10
			I-T-V R0 (60:8:32)	8%	10			I-T-V R0 (60:8:32)	9%	10
			I-T-V R0 (83:17)	32%	10			I-T-V R0 (83:17)	33%	10
			Illite	10%	14			Illite	9%	14
			I-V R1 (62:38)	6%	10			I-V R1 (62:38)	8%	10
(1E)_NH_4_D_Na	43%	14.09%	Kaolinite	10%	18	49%	16.71%	Kaolinite	9%	18
			I-T-V R0 (3:10:87)	5%	10			I-T-V R0 (3:9:88)	4%	10
			I-T-V R0 (20:32:48)	20%	10			I-T-V R0 (19:32:49)	20%	10
			I-T-V-S R0 (3:9:63:25)	9%	10			I-T-V-S R0 (3:8:64:25)	8%	10
			I-T-V R0 (60:16:24)	15%	10			I-T-V R0 (60:15:25)	14%	10
			I-T-V R0 (83:7:10)	32%	10			I-T-V R0 (83:8:9)	35%	10
			Illite	9%	14			Illite	10%	14

RH - relative humidity measued during XRD analysis
Rp - parameter describing the goodness of fit
[a] - I - illite, T - tobelite, V - vermiculite (accomodates one layer of water molecules within interlayers), S - smectite (accomodates two layers of water molecules within interlayers. The R0 and R1 denote random and ordered (exhibit MPDO) mixed layer phases phases, respectively. The numbers in brackets denote the relative proportions of illite *vs.* vermiculite *vs.* smectite within individual mixed layer minerals.
EG - ethylene glycol solvated samples
[b] - I - illite, T - tobelite, V - vermiculite (acomodating one layer of ethylene glycol molecules within interlayer space), S - smectite (accomodating two layers of ethylene glycol molecules within interlayer space, R0 and R1 denotes random and ordered (exhibiting MPDO) mixed layer phases phases respectively, numbers in brackets denote relative proportion of illite *vs.* vermiculite versus smectite within individual mixed layer minerals.
T mean - the mean cystallite thickness given in number of layers.

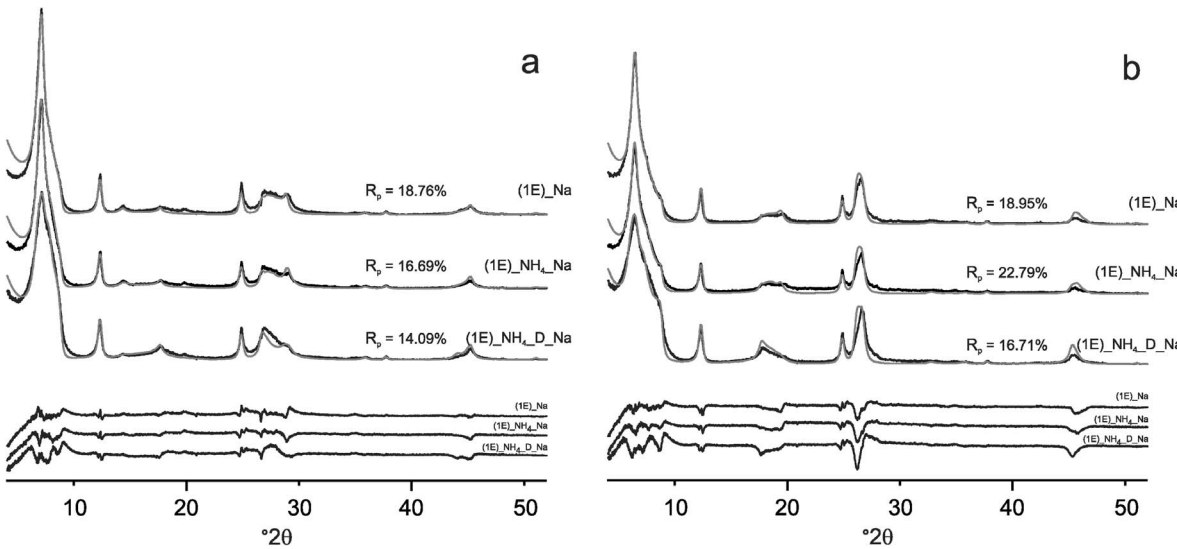

Figure 6. Experimental (black) and calculated (gray) XRD patterns of the solid products of the experiments (Table 1) using sample 1E: a) air-dried sample and (b) ethylene glycol-solvated sample. The difference XRD plots (modeled XRD pattern subtracted from XRD pattern) are shown at the bottom of each figure.

(Figure 7). Fixation of K^+ by dioctahedral vermiculite seemed to prevail over NH_4^+-fixation. Despite more intense K^+ than NH_4^+ fixation, the similar degree of interlayer collapse that occurred in both experiments implies that sample properties rather than the specific exchange cation control the extent of fixation. The layer charge range of the particular vermiculite must be sufficient to bind cations of low hydration enthalpy despite the substantially different K^+ and NH_4^+ charge densities (K^+ and NH_4^+ have similar hydration enthalpies, but NH_4^+ is a larger cation than K^+). These conclusions perfectly matched the results of Šucha and Širáňová (1991) who used multiple wetting and drying cycles with NH_4^+- and K^+-saturated smectites. The highest degree of fixation, which was close to 50% of all the layers for both cations, was obtained for a smectite with layer charge of ~0.6 and the degree of fixation was, in general, linearly dependent on the layer charge of the particular smectite.

As was done in the K-saturated sample, the XRD patterns of the Na-saturated sample (sample (1E)_NH_4Na), which was NH_4^+ saturated, kept moist, and then re-saturated with Na^+, were modeled using the starting models (*i.e.* those obtained by Skiba (2013) for

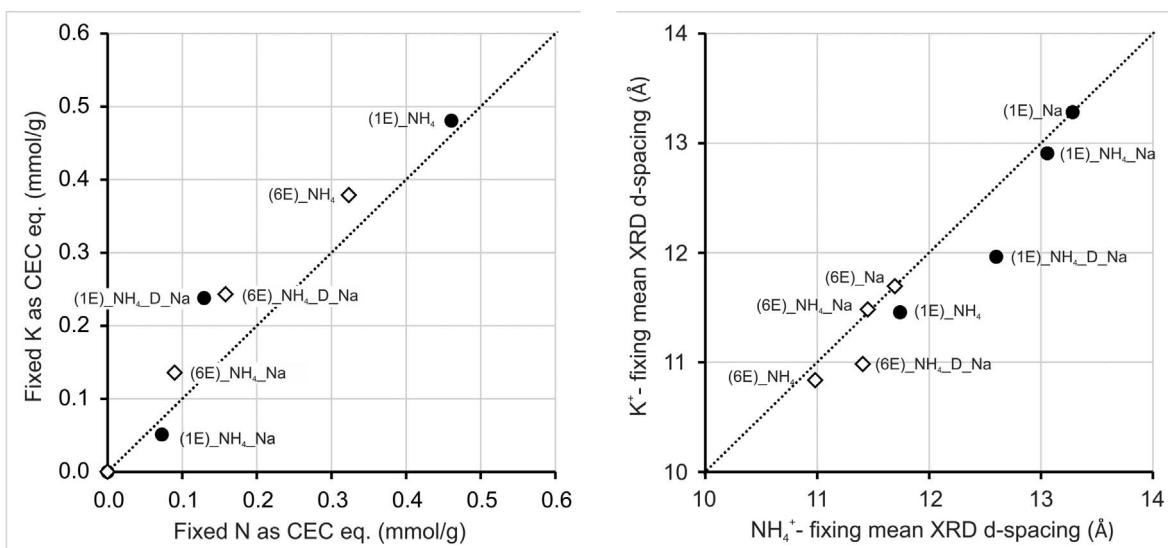

Figure 7. Potassium *vs.* NH_4^+ fixation presented as chemical data (left, after the cation exchange capacity values were recalculated as the equivalent fractions of fixed K and fixed NH_4) and as the mean XRD *d*-spacing (right) for experiments using the same samples from this study and from Skiba (2013 and unpublished data). The filled circles = sample 1E and the open diamonds = sample 6E.

https://doi.org/10.1346/CCMN.2018.064082 Published online by Cambridge University Press

sample (1E)_Na) using an increased amount of tobelite layers. The misfit values for the models were high (Figure 6) and similar to those obtained in a previous study for the corresponding XRD patterns. The tobelite concentrations calculated using the models were 3% and 2.8% for the air-dry and ethylene-glycol-solvated samples, respectively, The tobelite concentrations were close to but slightly lower than the values calculated for illite (3.1% and 3.9%, respectively) in a corresponding experiment that involved K^+-saturation (Skiba, 2013). The tobelite values were in good agreement with the chemical data (Figure 7). Five mixed-layer phases plus discrete illite and kaolinite were needed to model the XRD patterns of the NH_4-saturated, dried, and Na^+-re-saturated sample ((1E)_NH_4_D_Na), whereas XRD patterns of a K^+-saturated sample from a corresponding experiment (sample (1E)_K_D_Na) from Skiba (2013) were modeled using three mixed-layer phases plus discrete kaolinite and two populations of discrete illite. Calculated tobelite concentrations using those models were 11.7% and 11.4% for air-dry and ethylene-glycol-saturated samples, respectively. The values were significantly lower than the values for illite (20.41% and 20.06%, respectively) calculated in a corresponding experiment that used a K^+-saturated sample (Skiba, 2013). The observed differences were also in good agreement with the chemical data (Figure 7). For the (1E)_NH_4_D_Na sample, including some small admixtures of vermiculite-rich illite-tobelite-vermiculite phases was necessary to obtain a satisfactory fit between experimental and calculated patterns. For the (1E)_K_D_Na sample XRD patterns, the fit obtained used only illite-rich phases. In both cases (*i.e*. samples (1E)_NH_4_D_Na and (1E)_K_D_Na), the models used were much simpler than the starting (*i.e*. those used for the modeling the (1E)_Na sample) models, which indicates the transformation of illite-vermiculite and illite-vermiculite-smectite toward discrete illite and/or illite-tobelite.

Results of both of the independently performed chemical and XRD analyses indicated that K^+-fixation by dioctahedral vermiculite was more pronounced than NH_4^+-fixation. This finding is in good agreement with the general picture presented by Sawhney (1972) in which selective K^+ sorption and fixation by clays is stronger than NH_4^+ sorption and fixation.

Likely transformations of dioctahedral vermiculites in soils and diagenetic environments

The collapse of dioctahedral vermiculite due to NH_4^+ fixation was achieved in the present study using simplified laboratory systems. Despite this, the results still might be used, at least to a certain point, to discuss dioctahedral vermiculite transformation processes that likely take place in soils and sediments.

Dioctahedral vermiculite formed in soils is likely to transform into an NH_4-illite like phase when the NH_4^+ concentration is increased. This may happen both in soils and in organic-rich sediments due to organic matter decomposition/transformation processes that lead to the formation of NH_4^+ ions (Nieder *et al*., 1995). This also may take place in arable soils due to the addition of NH_4^+-based N fertilizers. This conclusion agrees well with field studies on NH_4^+ fixation by vermiculite-bearing soils treated with NH_4 fertilizers (*e.g*., Nieder *et al*., 2011; Matocha *et al*., 2016). According to Matocha *et al*. (2016), NH_4^+ fixation led to the formation of an NH_4-illite like phase identified by an increase in the intensity of the ~10 Å reflection, which was observed in soils extensively treated with NH_4-nitrate. The N in the soil clay fractions that were used as starting materials in the present study and the absorption bands characteristic of interlayer NH_4^+ in the FTIR spectra indicate that NH_4^+ fixation (leading to formation of an NH_4^+-illite-like phase) likely takes place in the soils of the Tatra Mountains. Because the soils have most likely never been fertilized, the fixed NH_4^+ clearly must have originated from natural soil processes of organic matter decomposition. The data available in the published research seem to support this conclusion because dioctahedral vermiculite-bearing soil clay fractions commonly show significant N concentrations and the FTIR spectra contain bands indicative of interlayer NH_4^+ (*e.g*. Bain and Fraser, 1994; Skiba, 2007). Fixation of the NH_4^+ that originated from soil organic matter mineralization was also reported by Nieder *et al*. (1995).

Ammonium fixation that leads to the collapse of dioctahedral vermiculite *via* interlayer dehydration appears to be a likely mechanism for the so called "soil illitization" reported in several studies (*e.g*. Berkgaut *et al*., 1994; Righi *et al*., 1995). This is likely to be especially true for soils that are rich in organic materials where NH_4^+ is expected to be produced by natural processes of organic matter decomposition. This kind of phenomenon involves the fixation of NH_4^+ from soil components and was reported by Nieder *et al*., (1995). The previously proposed and quite well-documented mechanisms that explain "soil illitization" involve K^+-fixation by dioctahedral vermiculite, which leads to interlayer collapse (Skiba, 2013). Cyclic wetting and drying cycles of K^+- and/or NH_4^+-saturated smectite and the reduction of smectite octahedral Fe(III) to Fe(II) (Eberl *et al*., 1986; Šucha and Širáňová, 1991; Shen and Stucki, 1994; Stucki, 2011) also contribute to interlayer collapse. Based on published data and the data presented in this study, one may conclude that the collapse of dioctahedral vermiculite and smectite interlayers due to both K^+ and NH_4^+ fixation can likely contribute to soil illite or tobelite formation. In soils that formed in climates that are not arid or semi-arid, interlayer collapse of dioctahedral vermiculite due to NH_4^+ (especially in organic-rich soils) and/or K^+ fixation is by far more likely to occur than smectite interlayer collapse due to wetting and drying. This is because of two reasons: (1) the

https://doi.org/10.1346/CCMN.2018.064082 Published online by Cambridge University Press

soils are rich in aluminous dioctahedral vermiculite (Douglas, 1989) and (2) drying does not very frequently occur in those soils. In soils of temperate climates, however, this mechanism would likely be mainly limited to the top soil horizons/soil surfaces and those are the only places where the relative humidity could become sufficiently low to dry the soil material.

Dioctahedral vermiculite is expected to occur in sedimentary basins because it is abundant in soils and its 2:1 layers are geochemically as stable as illite. Based on the available published data, however, dioctahedral vermiculite has never been reported in rocks and marine sediments. The immediate collapse of dioctahedral vermiculite interlayers and the presence of K^+ or NH_4^+ cations is the most probable mechanism to explain the lack of dioctahedral vermiculite in sedimentary systems.

CONCLUSIONS

The saturation of dioctahedral vermiculite exchange sites with NH_4^+ at room temperature collapsed it to a ~10.3 Å NH_4-illite-like phase. The collapse was irreversible to standard ion exchange treatments. The degree of NH_4^+-fixation observed in the present study was less pronounced than the degree of K^+-fixation produced for the same samples by Skiba (2013) in similar experiments. The observed interlayer collapse indicated that the process of NH_4^+-fixation that leads to the formation of an NH_4-illite-like phase at the expense of dioctahedral vermiculite very likely occurs in soils during weathering and in diagenetic environments because organic matter decomposition likely increased the NH_4^+ concentration. Both dioctahedral vermiculite and smectite interlayer collapse due to wetting and drying cycles and/or to octahedral Fe(III) to Fe(II) reduction can likely contribute to the formation of an NH_4-illite-like phase in soils. These processes need to be considered in studies that deal with the clay mineralogy of sedimentary basins.

ACKNOWLEDGMENTS

The authors thank Joseph W. Stucki, William Jaynes, Chris Matocha, Lukasz Uzarowicz, the associate editor, and the two anonymous reviewers for critical reading of the manuscript and for constructive suggestions and comments. William Jaynes and Chris Matocha also improved the English of the manuscript. Chevron ETC and Douglas McCarty are acknowledged for their permission to use their proprietary SYBILLA software. The present research was supported by Polish Ministry of Science and Higher Education Grant No. NN 305 379238.

REFERENCES

Ahlrichs, J., Fraser, A., and Russell, J. (1972) Interaction of ammonia with vermiculite. *Clay Minerals*, **9**, 263–273.

Bailey, S.W. (1980) Structures of Layer Silicates. Pp 2–124 in: *Crystal Structures of Clay Minerals and Their X-ray Identification* (G.W. Brindley and G. Brown, editors). Monograph 5, Mineralogical Society, London.

Bain, D.C. and Fraser, A.R. (1994) An unusually interlayered clay mineral from the eluvial horizon of a humus-iron podzol. *Clay Minerals*, **29**, 69–76.

Barnishel, R.I. and Bertsch, P.M. (1989) Chlorites and hydroxy-interlayered vermiculite and smectite. Pp. 729–788 in: *Minerals in Soil Environments 2nd edition* (J.B. Dixon and S.B. Weed, editors). Soil Science Society of America, Madison, Wisconsin.

Berkgaut, V., Singer, A., and Stahr, K. (1994) Palagonite reconsidered: Paracrystalline illite – smectites from regoliths on basic pyroclastics. *Clays and Clay Minerals*, **42**, 582–592.

Brown, G. (1953) The dioctahedral analogue of vermiculite. *Clay Minerals*, **2**, 67–70.

Brown, G. and Brindley, G.W. (1980) X-ray diffraction procedures for clay mineral identification. Pp 305-360 in: *Crystal Structures of Clay Minerals and Their X-ray Identification* (G.W. Brindley and G. Brown, editors). Monograph 5, Mineralogical Society, London.

Dolcater, D.L., Jackson, M.L., and Syers, J.K. (1972) Cation Exchange selectivity in mica and vermiculite. *American Mineralogist*, **57**, 1823–1831.

Douglas, L.A. (1989) Vermiculites. Pp 635–668 in: *Minerals in Soil Environments 2nd edition* (J.B. Dixon and S.B. Weed, editors). Soil Science Society of America, Madison, Wisconsin, USA.

Drits, V.A., Lindgreen, H., and Salyn, A.L. (1997) Determination of the content and distribution of fixed ammonium in illite-smectite by X-ray diffraction: Application to North Sea illite-smectite. *American Mineralogist*, **82**, 79–87.

Drits, V.A. and Sakharov, B.A. (1976) *X-ray Analysis of Mixed-layered Clay Minerals*. Nauka, Moscow (in Russian).

Drits, V.A., Sakharov, B.A., Salyn, A.L., and Lindgreen, H. (2005) Determination of the content and distribution of fixed ammonium in illite-smectite using a modified X-ray diffraction technique: Application to oil source rocks of western Greenland. *American Mineralogist*, **90**, 71–84.

Eberl, D. D., Środoń, J., and Northrop, H. R. (1986) Potassium fixation in smectite by wetting and drying. Pp. 296-326 in: *Geochemical Processes at Mineral Surfaces* (J.A. Davis and K.F. Hayes, editors). American Chemical Society Symposium Series v. 323.

Guggenheim, S., Adams, J.M., Bain, D.C., Bergaya, F., Brigatti, M.F., Drits, V.A., Formoso, M.L.L., Galan, E., Kogure, T., and Stanjek, H. (2006) Summary of recommendations of nomenclature committees relevant to clay mineralogy: Report of the Association Internationale pour L'Etude des Argiles (AIPEA) Nomenclature committee for 2006. *Clays and Clay Minerals*, **54**, 761–772.

Heller-Kallai, L. and Eberl, D. D. (1997) Potassium fixation by smectites in wetting-drying cycles with different anions. pp. 561–567 in: *Clays For Our Future*: *Proceedings of the 11th International Clay Conference, Ottawa, Canada, June 15–21, 1997*, (H. Kodama, A.R. Mermut, and J.K. Torrance, editors), ICC97 Organizing Committee, 1997.

Howard, S.A. and Preston, K.D. (1989) Profile fitting of powder diffraction patterns. Pp 217–275 in: *Modern Powder Diffraction* (D.L. Bish and J.E. Post, editors). Mineralogical Society of America, Chantilly, Virginia.

Jackson, M.L. (1969) *Soil Chemical Analysis. Advanced Course*, *2nd edition.* Published by the author, Madison, Wisconsin.

Matocha, J.C., Grove, J.H., Karathanasis, T.D., and Vandiviere, M. (2016) Changes in soil mineralogy due to nitrogen fertilization in an agroecosystem. *Geoderma*, **263**, 176–184.

Mehra, O.P. and Jackson, M.L. (1958) Iron oxide removal from soils and clays by dithionite – citrate system buffered with

sodium bicarbonate. *Clays and Clay Minerals*, **7**, 317–327.
Mesto, E., Scordari, F., Lacalamita, M., and Schingaro, E. (2012) Tobelite and NH_4^+-rich muscovite single crystals from Ordovician Armorican sandstones (Brittany, France): Structure and crystal chemistry. *American Mineralogist*, **97**, 1460–1468.
Moore, D.M. and Reynolds, R.C. (1997) *X-ray Diffraction and the Identification and Analysis of Clay Minerals 2nd edition.* Oxford University Press, USA.
Nieder, R., Dinesh, K.B., and Scherer, W. (2011) Fixation and defixation of ammonium in soils: A review. *Biology and Fertility of Soils*, **47**, 1–14.
Nieder, R., Willenbockel, A., Neugebauer, E., Widmer, P., and Richter, J. (1995) Die rolle der mikrobiellen biomasse und des mineralisch fixierten ammoniums bei den stickstoff-transformationen in niedersächsischen Löβ-Ackerböden unter Winter-Weizen. II. Umsetzung von ^{15}N-markiertem stickstoff. *Zeitschrift für Pflanzenernährung und Bodenkunde*, **158**, 477–484.
Petit, S., Righi, D., Madejova, J., and Decarreau, A. (1998) Layer charge estimation of smectites using infrared spectroscopy. *Clay Minerals*, **33**, 579–591.
Rich, C.I. (1964) Efect of cation size and pH on potassium exchange in Nanso soil. *Soil Science*, **98**, 100–105.
Rich, C.I. and Black, W.R. (1964) Potassium exchange as affected by cation size, pH, and mineral structure. *Soil Science*, **97**, 384–390.
Rich, C.I. and Obenshain, S.S. (1955) Chemical and clay mineral properties of a red-yellow podzolic soil derived from muscovite schist. *Soil Science Society of America Journal*, **19**, 334–339.
Righi, D., Velde, B., and Meunier A. (1995) Clay stability in clay-dominated soil systems. *Clay Minerals*, **30**, 45–54.
Russell, J.D. and Fraser, A.R. (1994). Infrared methods. Pp.11–64 in: *Clay Mineralogy: Spectroscopic and Chemical Determinative Methods* (M.J. Wilson, editor). Chapman & Hall, London.
Sawhney, B.L. (1972). Selective sorption and fixation of cations by clay minerals: A review. *Clays and Clay Minerals*, **20**, 93–100.
Shen, S. and Stucki, J.W. (1994) Effect of iron oxidation state on the fate and behavior of potassium in soils. Pp. 173–185 in: *Soil Testing: Prospects for Improving Nutrient Recommendations* (J.L. Havlin and J. Jacobsen, editors). Soil Science Society of America Special Publication Number 40, Soil Science Society of America, Madison. Wisconsin.
Skiba, M. (2007) Clay mineral formation during podzolization in an alpine environment of the Tatra Mountains, Poland. *Clays and Clay Minerals*, **55**, 618–634.
Skiba, M. (2013) Evolution of dioctahedral vermiculite in geological environments-An experimental approach. *Clays and Clay Minerals*, **61**, 290–302.
Skiba, M. and Skiba, S. (2005) Chemical and mineralogical index of podzolization of the granite regolith soils. *Polish Journal of Soil Science*, **38**, 153–162.
Skiba, M., Szczerba, M., Skiba, S., Bish, D.L., and Grybos, M. (2011) The nature of interlayering in clays from a podzol (spodosol) from the Tatra Mountains, Poland. *Geoderma*, 160, 425–433.
Stone, M. and Wild, A. (1978) The reaction of ammonia with vermiculite and hydrobiotite. *Clay Minerals*, **13**, 337–350.
Stucki, J.W. (2011) A review of the effects of iron redox cycles on smectite properties. *Comptes Rendus Geoscience*, **343**, 199–209.
Środoń, J. (1999) Use of clay minerals in reconstructing geological processes: Recent advances and some perspective. *Clay Minerals*, **34**, 27–37.
Środoń, J. and Gaweł, A. (1988) Identyfikacja rentgenograficzna mieszanopakietowych krzemianów warstwowych. Pp 290–307 in: *Metody Badań Mineralów i Skał* (A. Bolewski and W. Żabiński, editors). Wydawnictwa Geologiczne, Warsaw.
Środoń, J., Elsass, F., McHardy, W.J., and Morgan, D.J. (1992) Chemistry of illite/smectite inferred from TEM measurements of fundamental particles. *Clay Minerals*, **27**, 137–158.
Środoń, J., Zeelmaekers, E., and Derkowski, A. (2009) Charge of component layers of illite-smectite in bentonites and the nature of end-member illite. *Clays and Clay Minerals*, **57**, 650–672.
Šucha, V. and Širáňová, V. (1991) Ammonium and potassium fixation in smectite by wetting and drying. *Clays and Clay Minerals*, **39**, 556–559.
Viennet, J.C., Hubert, F., Ferrage, E., Terte, E., Legout, A., and Turpault, M.P. (2015). Investigation of clay mineralogy in a temperate acidic soil of a forest using X-ray diffraction profile modeling: Beyond the HIS and HIV description. *Geoderma*, **241**, 75–86.

(*Received 16 May 2017; revised 19 December 2017; Ms. 1181; AE: E. Garcia-Romero*)